Available online at www.sciencedirect.com
SCIENCE DIRECT
ELSEVIER
Geomorphology 74 (2006) 257–270
GEOMORPHOLOGY
www.elsevier.com/locate/geomorph

Evolution of the Bonneville shoreline scarp in west-central Utah: Comparison of scarp-analysis methods and implications for the diffusion model of hillslope evolution

J.D. Pelletier *, S.B. DeLong, A.H. Al-Suwaidi, M. Cline, Y. Lewis, J.L. Psillas, B. Yanites

Department of Geosciences, The University of Arizona, 1040 E. Fourth St., Tucson, AZ 85721, USA

Received 12 April 2005; received in revised form 17 August 2005; accepted 18 August 2005
Available online 11 October 2005

Abstract

Wave-cut pluvial shoreline scarps are ideal natural experiments in hillslope evolution because the ages of these scarps are often precisely known and because they form with a range of heights, alluvial textures, and microclimates (i.e., orientation). Previous work using midpoint-slope methods on pluvial scarps in the Basin and Range concluded that scarp evolution is nonlinear and microclimatically controlled. The purpose of this study was to further examine the influence of scarp height, texture and microclimate in an attempt to calibrate a nonlinear model of scarp evolution. To do this, over 150 profiles of the Bonneville shoreline in the adjacent Snake and Tule Valleys, west-central Utah were collected and analyzed by fitting the entire scarp profile to diffusion-equation solutions, taking into account uncertainty in the initial scarp angle. In contrast to previous studies, this analysis revealed no evidence for nonlinearity or microclimatic control. To understand the reason for this discrepancy, we undertook a systematic study of the accuracy of each scarp-analysis method. The midpoint-slope-inverse method was found to yield biased results, with systematically higher diffusion ages for young, tall scarps. The slope-offset method is unbiased but has limited resolution because it requires many scarp profiles to yield a single diffusion age. A method that incorporates the full scarp profile and uncertainty in the initial scarp angle was found to be the most accurate technique. The application of the full-scarp method to the Bonneville shoreline supports the use of a linear diffusion model for scarps up to 20 m in height. Scarp orientation had no discernable effect on diffusivity values. Soil texture was found to have a weak but significant inverse relationship with diffusivity values.

Keywords: Hillslope; Pluvial; Diffusion model; Basin and range; Scarp evolution

1. Introduction

Pluvial scarps have played a central role in research on hillslope geomorphology in arid regions throughout the world (Enzel et al., 1994; Hanks, 2000). Pluvial shoreline scarps form by wave-cut action during a prolonged period of lake-level high stand. Following lake-level fall, scarps formed in unconsolidated alluvium evolve to an "angle of repose" by mass movements and then further evolve by diffusive hillslope processes (Wallace, 1977). If a linear relationship between sediment flux (F) and slope is assumed:

$$F = \kappa \frac{\partial h}{\partial x} \tag{1}$$

where h is elevation, κ is diffusivity, and x is distance along a profile, then the scarp evolves from the angle

* Corresponding author.
E-mail address: jon@geo.arizona.edu (J.D. Pelletier).

0169-555X/$ - see front matter © 2005 Elsevier B.V. All rights reserved.
doi:10.1016/j.geomorph.2005.08.008

of repose according to the classic linear diffusion equation:

$$\frac{\partial h}{\partial t} = \frac{\partial F}{\partial x} = \kappa \frac{\partial^2 h}{\partial x^2} \quad (2)$$

where t is time. Measured scarp profiles may be compared to solutions of Eq. (2) in order to infer the scarp diffusion age, κT, where T is the scarp age.

Morphologic scarp analysis was pioneered by Bucknam and Anderson (1979), Nash (1980a,b, 1984), Hanks et al. (1984), and Hanks and Wallace (1985). Using well-dated, late glacial pluvial scarps in the Basin and Range, values for κ between 0.1 and 10 m^2/kyr were calculated. These κ values have then been used in regional paleoseismic studies (e.g., Pearthree and Calvo, 1987). Pluvial scarps can also be used to test alternative mathematical models of hillslope evolution (i.e., linear vs. nonlinear diffusion).

As shown in Eq. (1), the linear diffusion model for hillslope evolution, first proposed by Culling (1960, 1963), assumes that the flux of material is proportional to the hillslope gradient. This model is most appropriate for unconsolidated alluvium with low gradients. Hillslope processes that can be approximated with the diffusion equation include creep, bioturbation and rainsplash on low-gradient slopes. Slope wash is not included in this list because sediment transport by slope wash increases with distance from the divide, leading to diffusivity values that vary along the length of the slope (Carson and Kirkby, 1972; Hallet and Putkonen, 1994). Application of the diffusion equation to creep processes has theoretical support from the particle-based model developed by Furbish and Haff (1999). Cosmogenic-isotope studies have also provided empirical support for the diffusion model in certain environments (e.g., McKean et al., 1993; Heimsath et al., 1997). For steep slopes, it is well understood that the diffusion equation does not apply (e.g., Roering et al., 1999; Martin, 2000).

A fundamental uncertainty in scarp analysis is the value of the initial scarp angle or gradient (Mayer, 1984). The initial gradient cannot be measured from the scarp itself because time has erased the initial condition. The initial gradient cannot readily be estimated because it depends on material texture, cohesion and other factors in a complex manner. For example, scarp orientation may affect the initial gradient because it affects evapotranspiration, pore pressure, slope stability, and hence, initial gradient. Even the angle of repose of dry, cohesionless sand varies between 28° and 42°, depending on grain size and angularity (Simons and Albertson, 1963). Variations in cohesion are likely to broaden this range considerably in real scarps, especially between scarps formed on alluvial deposits of different ages with variable soil material properties. The uncertainty in initial gradient should correspond directly to a numerical uncertainty in diffusion age, but techniques for incorporating quantitative uncertainty in scarp analysis on a profile-by-profile basis have only recently been implemented (e.g., Mattson and Bruhn, 2001). As a result, the impact of uncertainty in scarp initial conditions on the resulting diffusion ages, although widely recognized in previous studies, has not been quantitatively evaluated.

Scarp methods come in two basic types: midpoint-slope methods and full-scarp methods. Midpoint slope methods can be further divided into two basic types. In the first type, the midpoint slope of a single scarp is inverted for diffusion age using the analytic solution to the diffusion equation (Andrews and Hanks, 1985). In the second approach, the midpoint gradient is plotted vs. scarp offset for a collection of many scarps with different heights (Bucknam and Anderson, 1979; Hanks and Andrews, 1989). In this approach, the far-field gradient (i.e., the gradient far from the scarp) must first be subtracted from the midpoint gradient to take into account the effects of scarps cut into sloping surfaces. The plot of midpoint gradient (reduced by the far-field gradient) is compared against characteristic curves for the diffusion equation with different parameter values (e.g., Bucknam and Anderson, 1979; Hanks et al., 1984) to determine which parameters best match the observed data. Both methods are potentially unreliable because they reduce the information content of the scarp to the slope at a single point. The scarp midpoint is the least diagnostic point along the entire scarp profile, and it is the point that is also most sensitive to uncertainty in the initial scarp angle. As a scarp evolves, the greatest amount of aggradation and degradation occurs where the magnitude of the hillslope curvature is greatest, near the top and bottom of the scarp. The scarp midpoint is a point of inflection with zero curvature, and hence, this point changes the least of all points along the profile. An alternative approach is to fit the entire scarp (or its derivative, the hillslope gradient) to analytic or numerical solutions of the diffusion equation (linear or nonlinear). Avouac et al. (Avouac, 1993; Avouac and Peltzer, 1993) pioneered the use of this technique in fault-scarp studies in Asia. Mattson and Bruhn (2001) extended the technique to include uncertainty in the initial scarp angle. To date, however, no study has undertaken a systematic reassessment of the classic pluvial scarps of the Basin and Range based on these new techniques. This study is designed to fill that gap.

2. Previous work and open questions

The literature on scarp analysis has included a vigorous debate on linear vs. nonlinear diffusion models. For example, Andrews and Hanks (1985) proposed that the flux of material is proportional to the gradient for small values, but increases towards infinity as the gradient reaches a critical value S_c:

$$F = \kappa \frac{\partial h/\partial x}{1 - \left(\frac{|\partial h/\partial x|}{S_c}\right)^n} \quad (3)$$

where n is a constant. If this relationship is assumed, Eq. (2) becomes

$$\frac{\partial h}{\partial t} = \frac{\partial F}{\partial x} = \kappa \frac{\partial h/\partial x}{1 - \left(\frac{|\partial h/\partial x|}{S_c}\right)^n} \times \left[1 + \frac{n|\partial h/\partial x|^n}{S_c^n\left(1 - \left(\frac{|\partial h/\partial x|}{S_c}\right)^n\right)}\right]. \quad (4)$$

Andrews and Hanks (1985) proposed using Eq. (4) with $n=1$, while Andrews and Bucknam (1987) and Mattson and Bruhn (2001) assumed $n=2$. On the one hand, it may seem obvious that a nonlinear model should be used to model scarp evolution, since hillslope transport rates do increase as diffusive processes give way to mass-movement processes with increasing gradient. On the other hand, it is difficult to prove which particular nonlinear model is most applicable in any given environment. Eq. (4) is just one possible nonlinear model, and it remains to be shown whether scarp evolution in the Basin and Range follows this or any other specific nonlinear diffusion equation. Previous scarp studies have argued that nonlinearity is important for scarps of essentially all heights (e.g., empirical results of Pierce and Colman, 1986), a result inconsistent with the abrupt transition to nonlinearity represented in Eq. (4) as the gradient approaches S_c. There is an additional danger in using any nonlinear diffusion model without direct supporting evidence, because nonlinear models incorporate additional unconstrained model parameters that may lead to an under-determined inverse problem. In the nonlinear diffusion-model framework, for example, the diffusion age, the initial scarp gradient and the parameters of the nonlinear model (e.g., S_c and n in Eq. (4)) must all be determined by inversion from a single scarp or a collection of scarps. As the number of unconstrained parameters grows, however, the likelihood that a best-fit solution will accurately constrain any one particular parameter (i.e., diffusion age) decreases. If the goal is to extract the most accurate diffusion age, it is best to determine the form and parameter values of the nonlinear model from empirical evidence or from an understanding of hillslope processes and then apply the most appropriate model based on that evidence.

Pierce and Colman (1986) obtained perhaps the most widely cited evidence for nonlinearity and microclimatic control in scarp evolution. They used the maximum-slope-scarp-offset method to analyze Late Pleistocene fluvial terrace scarps in Idaho. Their study showed that diffusivity values varied locally by as much as a factor of 30 depending on scarp height and orientation. Despite the extensive analysis presented in their study, it should be noted that fluvial terrace scarps are fundamentally unreliable landforms for scarp analysis. It is commonly assumed that the morphologic age of a fluvial terrace scarp and the age of the terrace tread are equivalent (Pierce and Colman, 1986; Nash, 1984). Fluvial terrace scarps, however, do not record the age of entrenchment and terrace abandonment but instead record the last time the terrace scarp was eroded by a laterally migrating incised channel. Incised channels commonly widen by bank retreat following entrenchment, reworking deposits laterally and maintaining steep scarps in deposits of any age they encounter. This reworking can be spatially complex; a terrace may be recently reworked on one side of the channel and completely preserved on the other side. As a result, there may be no relationship between the terrace abandonment age and the time since the terrace scarp was last modified by non-diffusive processes (i.e., its morphologic age). Terrace scarps may not even be of uniform age on the same side of the channel (due to complex lateral migration patterns) or even within a single profile (i.e., reworking of the lower half by bank retreat may leave the top half unscathed). To avoid this problem, Hsu and Pelletier (2004) performed scarp analysis on gully slopes incised into the terrace interior. This technique requires that other conditions be met, however, specifically that gullies reach lateral and vertical stability soon after they form.

To corroborate their work in Idaho, Pierce and Colman (1986) also documented nonlinear evolution in the Bonneville shoreline scarp. Shoreline scarps do not suffer from the problems of terrace scarps discussed above. The maximum-slope scarp-angle method that they used, however, was subsequently updated to

account for the far-field gradient (the surface gradient far from the scarp), and no evidence for nonlinearity was detected (Hanks and Andrews, 1989). More recently, Mattson and Bruhn (2001) utilized a full-scarp method and did detect nonlinearity in Bonneville scarps greater than 20 m in height. The diversity of results from these studies leaves the question of linear or nonlinear evolution unresolved and suggests that a systematic analysis of the accuracy of each scarp method would be useful.

3. Study area and field methods

Our study area is the adjacent Snake and Tule Valleys of west-central Utah (Fig. 1). This area was chosen because Lake Bonneville cut deposits with a wide range of textures and orientations, forming scarps of 1–20 m in height, and because Tule Valley was mapped in detail by Sack (1990). Fig. 2 presents an oblique aerial view of the shoreline in east-central Tule Valley as it cuts across several distinct geomorphic surfaces. This figure illustrates that scarp height is controlled primarily by the slope of the deposit, with the tallest scarps formed in steeply dipping alluvial fan deposits and debris cones close to the mountain front. Scarps in the study area are predominantly oriented towards the east and west, but locally, there are also segments of south- and north-facing scarps. Wave-cut piedmont deposits are debris-flow dominated in this area. Debris-flow levees were observed in modern channels, and older deposits are comprised of matrix-supported, angular and poorly sorted deposits characteristic of debris flows.

Between December 2003 and February 2004, we measured over 150 profiles of the Bonneville shoreline using a pole-mounted laser rangefinder and theodolite. Profiles were obtained by positioning the rangefinder near the top of the scarp to ensure a

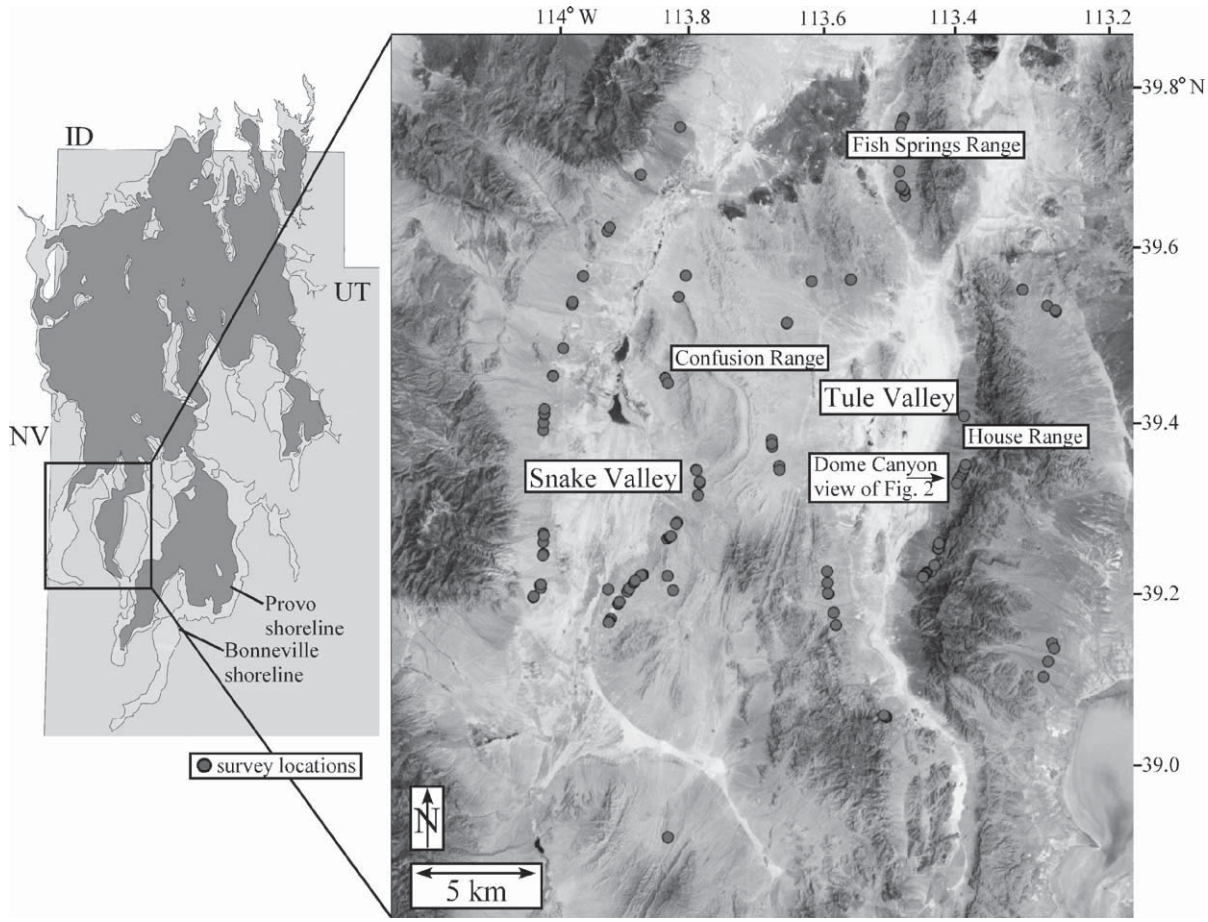

Fig. 1. Location map of study sites, Snake and Tule Valleys, southwestern Utah. The extent of Lake Bonneville at left is adapted from Reheis (1999). Landsat image is at right. Locations of survey stations are shown with circles.

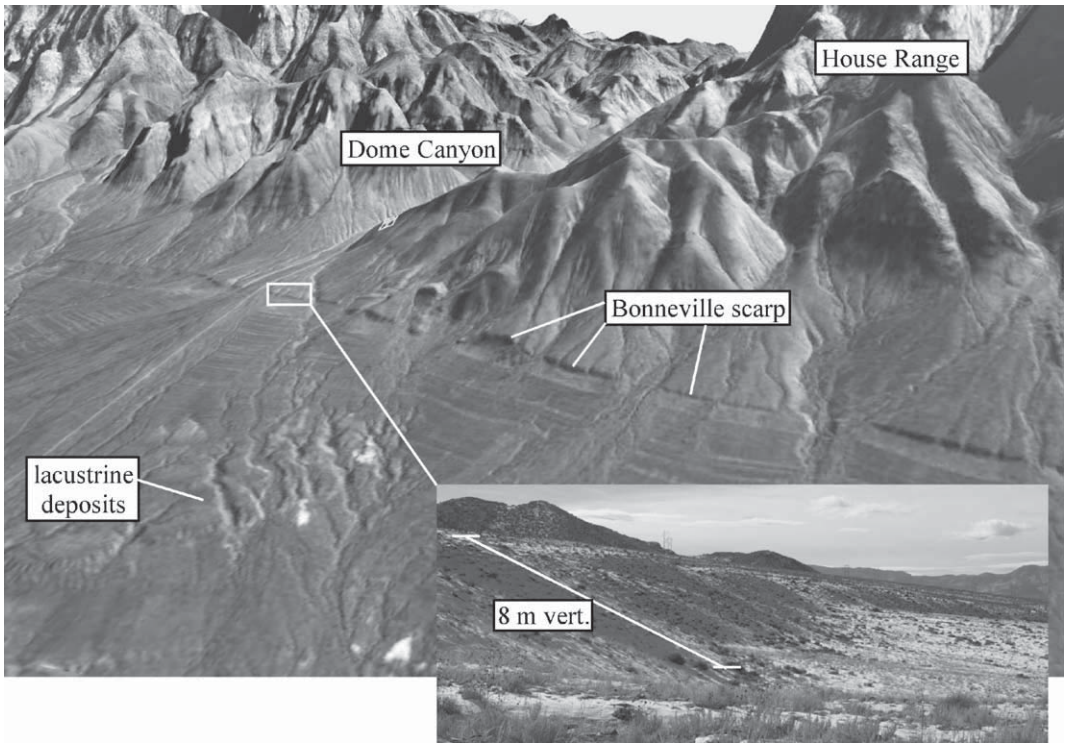

Fig. 2. Virtual oblique aerial photograph (i.e., aerial photo draped over digital topography) of pluvial features on the east side of central Tule Valley. Scarp height is primarily controlled by the slope of the alluvial-fan and debris-cone deposits, i.e., wave-cut erosion of steeply dipping deposits tends to produce steep, tall scarps. Inset photo shows 8-m-tall scarp at the entrance to Dome Canyon.

continuous line-of-sight upslope and downslope so that the entire profile could be acquired without moving the rangefinder mount. We took special care to continue each profile well past the upper and lower halves of each scarp in order to identify the far-field gradient accurately. Profile points were spaced between 0.5 and 2 m apart, depending on overall scarp length. At each scarp "station," two to four profiles were measured within close proximity to quantify profile-to-profile variability. Repeat profiles resulted in variations of approximately 5 cm, similar to the variability reported by Mattson and Bruhn (2001), who also used a laser rangefinder. This variability included measurement error and the effects of microtopography, including plant mounds, animal burrows and large clasts. Coarse, bouldery scarps yielded somewhat larger point-to-point variations ($\approx$10 cm) between repeat profiles. Scarp profiles were carefully chosen to avoid the effects of nearby gullies, which can lead to three-dimensional effects such as "crowning" of the upper half of the scarp and localized fan deposition at the bottom half. At each station, vegetation cover, scarp orientation, and the maximum and mean clast intermediate-axis diameters (averaged from 100 samples) were measured. Light snow cover on one field trip prevented the collection of textural data for all of the scarp stations.

4. Evaluation and comparison of scarp-analysis methods

4.1. Mathematical background

The geometry of a general scarp is defined by the scarp height $2a$, initial gradient α, and far-field gradient b (Fig. 3A). The initial and far-field gradients can be combined for the purposes of scarp analysis into a single variable: the reduced initial gradient $\alpha - b$. The analytic solution to the linear diffusion equation for a general scarp was given by Hanks and Andrews (1989) as

$$h(x,t) = (\alpha - b)\sqrt{\frac{\kappa t}{\pi}}\left(e^{-\frac{(x+a/(\alpha-b))^2}{4\kappa t}} - e^{\frac{(x-a/(\alpha-b))^2}{4\kappa t}}\right) + \frac{(\alpha-b)}{2}\left(\left(x+\frac{a}{\alpha-b}\right)\mathrm{erf}\left(\frac{x+a/(\alpha-b)}{\sqrt{4\kappa t}}\right) - \left(x-\frac{a}{\alpha-b}\right)\mathrm{erf}\left(\frac{x-a/(\alpha-b)}{\sqrt{4\kappa t}}\right)\right) + bx \quad (5)$$

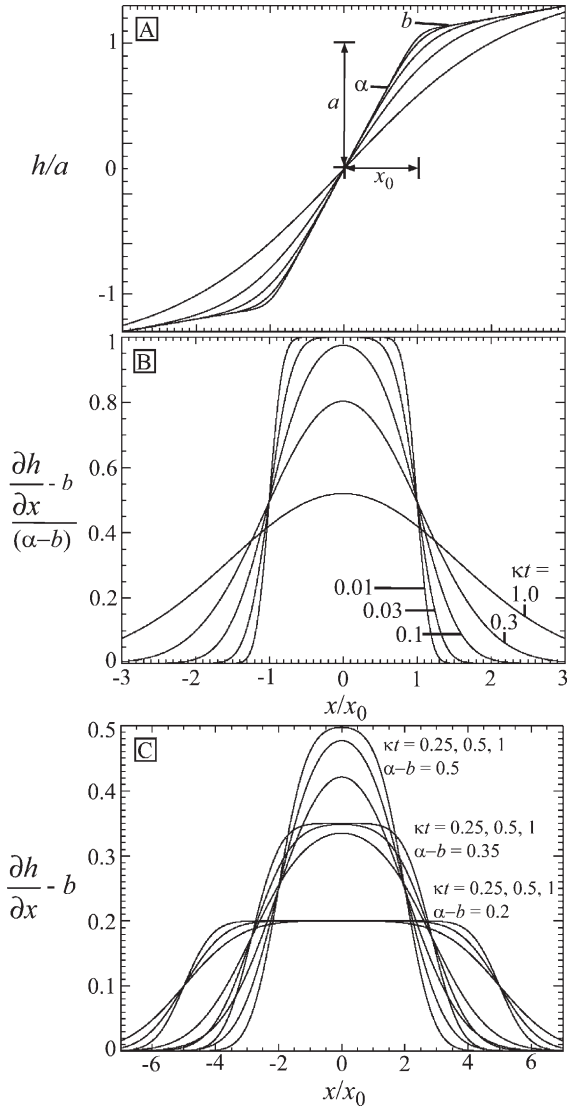

Fig. 3. (A) Analytic solutions of the linear diffusion equation, starting from an initial gradient α, scarp height $2a$, and far-field slope b. The initial scarp width, $2x_0$, is related to height and reduced initial gradient by $x_0=a/(\alpha-b)$. (B) Plots of reduced gradient corresponding to the profiles in (A). For small κt values (<0.1), no change in the midpoint slope is observed, illustrating the insensitivity of the midpoint slope to diffusion age for young scarps. (C) Plots of reduced gradient vs. distance along the profile, for families of solutions corresponding to a range of diffusion ages ($\kappa t=0.25,\ 0.5,\ 1$) and a range of reduced initial gradients ($\alpha-b=0.2,\ 0.35,\ 0.5$).

where erf is the error function. Full-scarp analyses can be performed by comparing the measured elevation profile of a scarp to Eq. (5), or by taking the derivative of the elevation profile and working with the slope or gradient profile. Working with the gradient profile is mathematically simpler because the derivative of Eq. (5) is a more compact expression:

$$\frac{\partial h(x,t)}{\partial x} - b = \frac{(\alpha-b)}{2}\left(\mathrm{erf}\left(\frac{x+a/(\alpha-b)}{\sqrt{4\kappa t}}\right) - \mathrm{erf}\left(\frac{x-a/(\alpha-b)}{\sqrt{4\kappa t}}\right)\right). \quad (6)$$

The left-hand side of Eq. (6) is called the reduced gradient profile (i.e., the gradient profile "reduced" by b, in order to take the far-field gradient into account as discussed in more detail below). Eqs. (5) and (6) are plotted in Fig. 3 for a range of diffusion ages κt and reduced initial scarp gradients, $\alpha-b$. Fig. 3B illustrates that the midpoint of the scarp is insensitive to age for young, tall scarps. Note that in Fig. 3, the units of the x-axis are scaled to the scarp width x_0, which, in turn, is scaled to the scarp height through the relationship $x_0=a/(\alpha-b)$. Fig. 3C illustrates that as the reduced initial gradient decreases, the age-diagnostic portion of the scarp becomes progressively concentrated away from the midpoint towards the top and bottom of the scarp. These plots suggest that full-scarp methods are necessary to extract the independent controls of scarp age and initial gradient on scarp morphology.

4.2. Midpoint-slope and slope-offset methods

The midpoint-slope-inverse method works with the reduced gradient of the scarp measured at the midpoint. In this method, Eq. (5) is evaluated at $x=0$ and inverted to obtain

$$\kappa T = \left(a \Big/ \left(2(\alpha-b)\mathrm{erf}^{-1}\left(\frac{\partial h/\partial x|_{x=0}-b}{\alpha-b}\right)\right)\right)^2. \quad (7)$$

Andrews and Hanks (1985) described this method somewhat differently in terms of moments, but the approach is the same. The far-field gradient can be measured directly in the field, but the initial scarp gradient α, needed to evaluate Eq. (7), must be assumed. A range of values for α have been used, with values between 30° and 35° being the most common. The 30–35° range is lower than the range observed for dry sand, so it may be unrealistically narrow for real scarps. The difference between 30° and 35° may seem small, but it is a very significant difference for young, tall scarps that require long periods of time to evolve significantly from the initial gradient.

We used Eq. (7) to compute the diffusivity of each of the Bonneville shoreline profiles measured in Snake

and Tule Valleys, assuming an initial scarp gradient of 0.6 (31°) and a scarp age of 15.4 ka (Oviatt et al., 1992). The initial scarp gradient was converted to a reduced scarp gradient unique to each profile using the far-field gradient measured in the field for each scarp. Then Eq. (6) was applied, using the midpoint gradient also measured in the field. The resulting diffusivity values are plotted in Fig. 4A as a function of scarp height. This plot shows a systematic increase in diffusivity values with increasing height. Twenty of the measured profiles had midpoint gradients greater than our assumed initial value of 0.6 and, hence, yielded "negative" ages. In Fig. 6, these points are plotted at the lowest point on the y-axis with the label "no finite value." To avoid these anomalous results, the assumed initial scarp gradient can be increased to a value greater than the steepest measured scarp in the region (Nash, 1980a). However, results described below indicate that increasing the assumed initial gradient also increases the likelihood of biased results.

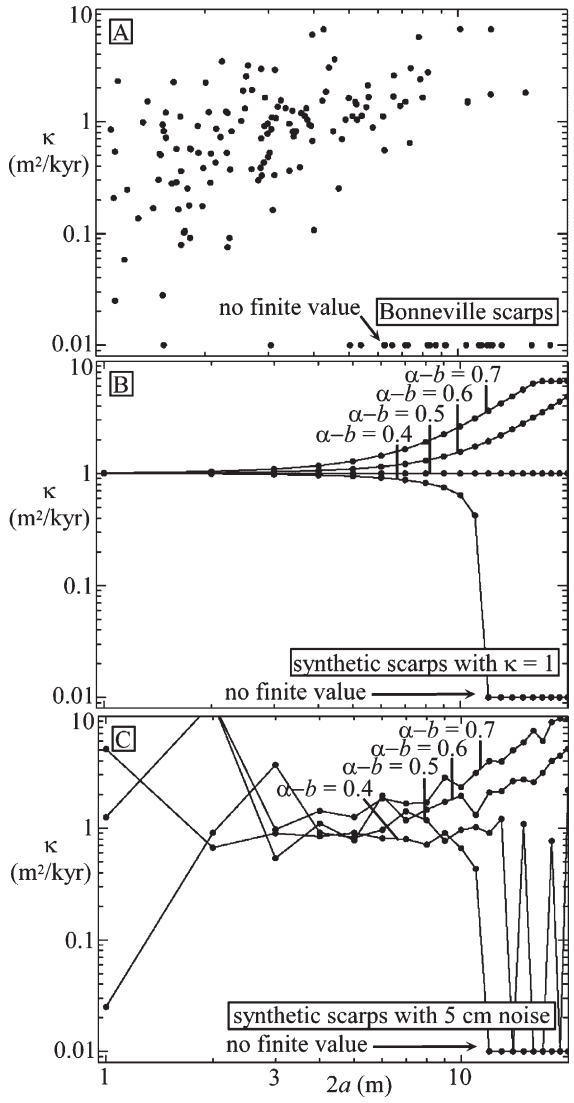

Fig. 4. Diffusivity values inferred from midpoint-slope-inverse method for (A) Bonneville scarps, (B) analytic solutions of the diffusion equation with $\kappa = 1$ m^2/kyr, $T = 10$ kyr, and a range of scarp heights ($2a = 1$–20 m) and initial gradients ($\alpha - b = 0.4$–0.7), and (C) analytic solutions (same as B), with small-scale (5-cm root-mean-squared) random variability superimposed. Scarps with midpoint gradients greater than the assumed initial value yield "negative" ages and are plotted here on the lowest point on the y-axis with the label "no finite value."

To evaluate the accuracy of the midpoint-slope-inverse method, we used Eq. (7) to calculate the diffusion age for synthetic profiles in which the diffusion age and initial gradient were precisely known. We used two types of synthetic profiles for this analysis: (1) analytic solutions of Eq. (5), and (2) the same profiles with small, 5-cm root-mean-squared, random variability superimposed. Random variability was included to make this analysis more relevant to actual scarps, which often include some small-scale variability or roughness due to local plant and animal disturbances (Jyotsna and Haff, 1997). Synthetic profiles were created using $\kappa = 1$ m^2/kyr, a scarp age of 10 ka, a reduced initial gradient of $\alpha - b = 0.6$ (i.e., $\alpha = 0.6$, $b = 0$), and a range of scarp heights. The initial gradient is unknown in real applications, so we have performed this analysis using a range of assumed reduced initial gradients, ranging from $\alpha - b = 0.4$ to $\alpha - b = 0.7$. Fig. 4B illustrates the results as a function of scarp height and assumed reduced initial gradient. As scarp height increases, the diffusivity values increase significantly relative to the correct answer, denoted by the horizontal line with $\kappa = 1$ m^2/kyr. These results illustrate that the midpoint-slope-inverse method yields biased diffusion ages for tall scarps, unless the initial angle is exactly known. Since the initial angle is generally unknown and somewhat variable from scarp to scarp, in practice this method will always produce biased results. In addition, it is dangerous to simply increase the assumed initial gradient in order to match the steepest scarp in a region (thereby avoiding "negative" ages), because unless all the scarps in a region have identical initial gradients, increasing the assumed angle to match the steepest scarp will have the effect of increasing the bias in this method for the remaining scarps. The bias will be particularly extreme if tall, steep scarps have initial gradients that are systematically greater than short, gentle scarps. Field observations in west-central Utah suggest that this is the case because tall, steep scarps were observed to form preferentially in coarse, angular

alluvial-fan deposits and debris cones. Coarse, angular sediments have systematically higher angles of repose (Simons and Albertson, 1963), and hence, their initial gradients are probably also larger.

Fig. 4C presents results of the same sequence of analyses with 5-cm root-mean-squared (RMS) random variability superimposed on the analytic solutions. As in Fig. 4B, the correct result is a horizontal line with $\kappa = 1$ m^2/kyr. These results indicate that random variability in scarp morphology results in a concomitant variability in diffusion ages. The presence of random variability, however, does not affect all scarps to the same extent: short scarps are particularly sensitive to small-scale variability, yielding diffusivity values more than an order of magnitude in error for scarps less than 3 m tall. This result suggests that problems with scarp-analysis methods cannot be avoided simply by analyzing short scarps, as suggested by Nash (1998), because the signal-to-noise ratio is lower in short scarps.

Bucknam and Anderson (1979) advocated plotting the relationship between the maximum slope and the scarp height for a collection of scarps in a given region. They noted that maximum scarp angle and scarp height have a strong linear correlation but are offset vertically from one another on a graph according to diffusion age. Hanks and Andrews (1989) improved this method by incorporating the far-field gradient. This method is referred to as the slope-offset method.

To evaluate the slope-offset method, we performed a set of analyses analogous to those shown in Fig. 4. The slope-offset method yields a single scatter plot of results rather than a unique value for each scarp. The diffusion age can be determined by fitting the scatter plot to characteristic curves for different diffusion ages and reduced initial gradients. This fitting can be done visually or formally using multivariate curve-fitting methods. The results for the Bonneville scarps are shown in Fig. 5A, along with characteristic curves corresponding to $\kappa = 1$ m^2/kyr and $\kappa = 2$ m^2/kyr, both assuming $\alpha - b = 0.6$. Comparing these two curves, $\kappa = 1$ m^2/kyr is clearly a better fit to the data, indicating that the method can determine the average diffusion age for a collection of scarps to within roughly a factor of 2. The disadvantage of this method is twofold: it has limited ability to determine the diffusion age uniquely, and it can only determine the average value for a collection of scarps since it cannot be applied on a profile-by-profile basis. The large scatter in the data for both short and tall scarps means that a range of initial gradients and diffusion ages are equally consistent with the data. The method also implicitly assumes that all scarps in the collection have the same diffusion age and initial gradient. Therefore, the method is not well suited to identifying local controls on diffusion age, such as texture and orientation, which would be better detected on a profile-by-profile basis.

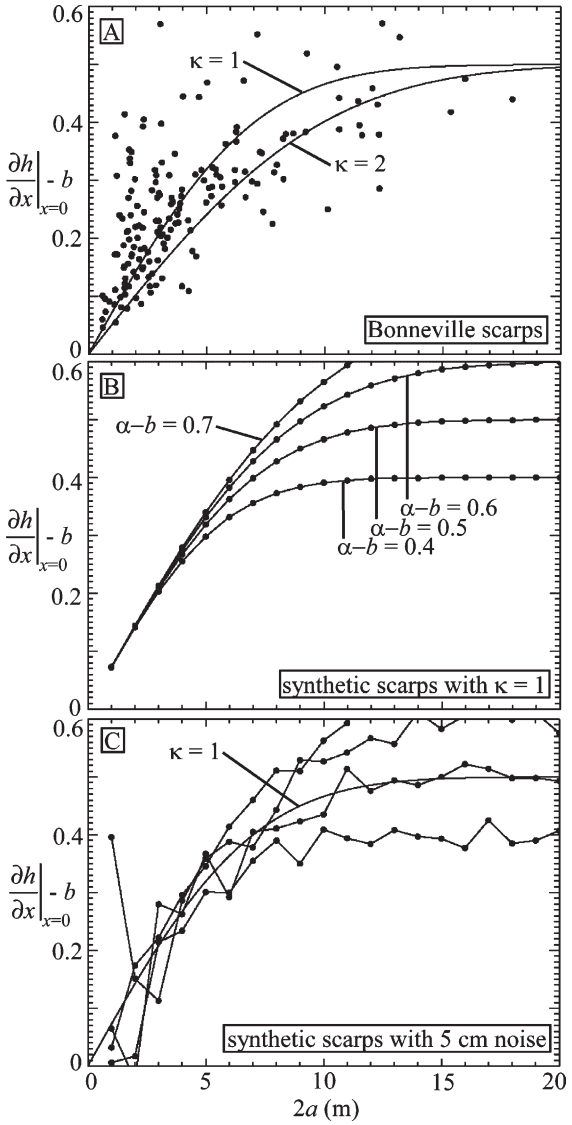

Fig. 5. Diffusivity values inferred from midpoint-slope-inverse method for (A) Bonneville scarps, (B) analytic solutions of the diffusion equation with $\kappa = 1$ m^2/kyr, $T = 10$ kyr, and a range of scarp heights ($2a = 1$–20 m) and reduced initial gradients ($\alpha - b = 0.4$–0.7), and (C) analytic solutions (same as B) with small-scale (5-cm root-mean-squared) random variability superimposed.

Fig. 5B illustrates the results of the slope-offset method for analytic solutions in the absence of noise. This method avoids the bias of the midpoint-slope-inverse method, because the plateau in the reduced

gradient for tall scarps provides an effective measure for the value of the reduced initial gradient. This method still assumes, however, that initial scarp angles are uniform and independent of scarp height, assumptions which are unlikely to hold for a collection of many scarps. The performance of this method in the presence of noise is illustrated in Fig. 5C. The method is able to detect the reduced initial gradient with considerable precision (assuming it is uniform, as in the synthetic data), but the small-scale variability presents a problem for uniquely determining the shape of the curve for scarps less than 3 m tall.

4.3. Full-scarp methods

As an alternative to midpoint-slope methods, the entire scarp profile can be fit to analytic or numerical solutions for a range of parameter values until an optimal fit is achieved. Two approaches can be used to find this optimal fit. First, a nonlinear, multivariate curve-fitting technique such as the Levenberg–Marquardt algorithm (Press et al., 1992) can be used to search for the best fit in an automated fashion. In this approach, the user prescribes estimated values for the initial gradient and diffusion age. The algorithm then

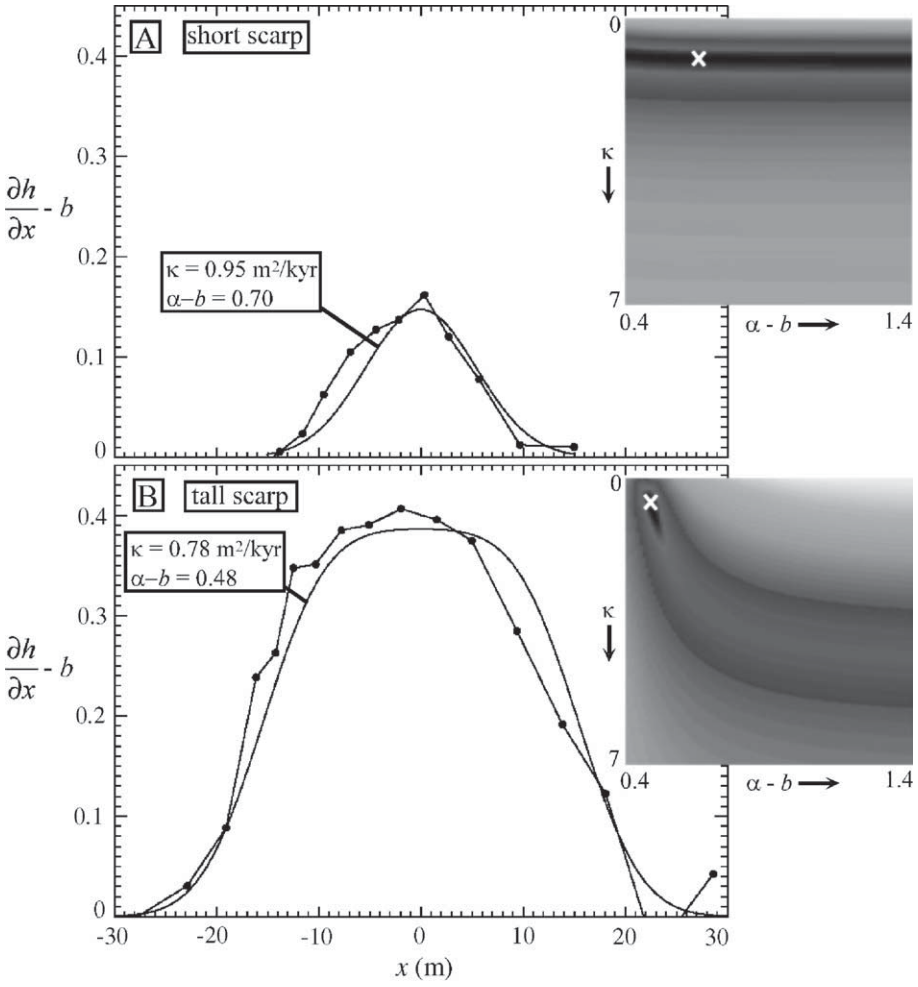

Fig. 6. Full-scarp curve-fitting method illustrated for (A) short and (B) tall example Bonneville scarps. The reduced gradient is plotted as a function of distance from the scarp midpoint. Grayscale maps to the right of each plot illustrate the relative error between the observed and modeled scarp as a function of diffusivity κ and reduced initial gradient $\alpha - b$. In both maps, black colors represent the lowest mismatch and X marks the spot of the optimal fit. The location of this best-fit solution in the model parameter space simultaneously determines diffusivity and reduced initial gradient on a profile-by-profile basis. In the short-scarp example case in (A), the best-fit solution corresponds to $\kappa = 0.95$ m^2/kyr and $\alpha - b = 0.70$. The black band running across the grayscale map illustrates that, although the best-fit solution occurs for $\alpha - b = 0.70$, the solution is essentially independent of the reduced initial gradient. This makes physical sense because, for a short, narrow scarp, diffusive smoothing quickly reduces the maximum slope to a value far below the angle of repose. For a tall, broad scarp (B), however, the solution is sensitive to the initial angle. The best-fit model parameters in this case have well-defined values for both diffusion age and reduced initial gradient ($\kappa = 0.78$ m^2/kyr and $\alpha - b = 0.48$).

calculates the difference between the model prediction and observed data (i.e., the model "error"), as well as the local derivatives of the error with respect to each parameter. Using a type of "smart" search based on the derivatives of the model error, the Levenberg–Marquardt algorithm narrows in on the best-fit parameter values. Alternatively, a brute-force approach can be used which computes analytic or numerical solutions corresponding to a full range of model parameters and then plots the error between the model and measured profiles as a function of each parameter value (e.g., diffusion age and initial gradient). The diffusion age is then constrained by the model profile that has the lowest error relative to the measured data. This brute-force approach is most often used, and it has the advantage that the goodness of fit can be evaluated visually on a profile-by-profile basis. Avouac (1993) and Arrowsmith et al. (1998) pioneered this technique, assuming initial scarp angles between 30° and 35°. Mattson and Bruhn (2001) improved upon this approach by including a range of initial gradients in the analysis. Mattson and Bruhn's error plots are thus two-dimensional, including a range of both diffusion age and reduced initial angle in the analysis.

Fig. 6A and B illustrates the full-scarp method on a short and a tall scarp, respectively, each selected from the set of Bonneville scarps. The reduced gradient is plotted as a function of distance along the profile. To the right of each plot is a grayscale map that illustrates the relative least-square error between the model and observed profiles for a range of diffusivity values and reduced initial gradients. In both maps, black colors represent the lowest mismatch and X marks the spot of the optimal fit. The location of this best-fit solution in the model parameter space simultaneously determines diffusivity and reduced initial gradient on a profile-by-profile basis. In the short-scarp example case, the best-fit solution corresponds to $\kappa = 0.95$ m^2/kyr and $\alpha - b = 0.70$. The black band running across the grayscale map illustrates that, although the best-fit solution

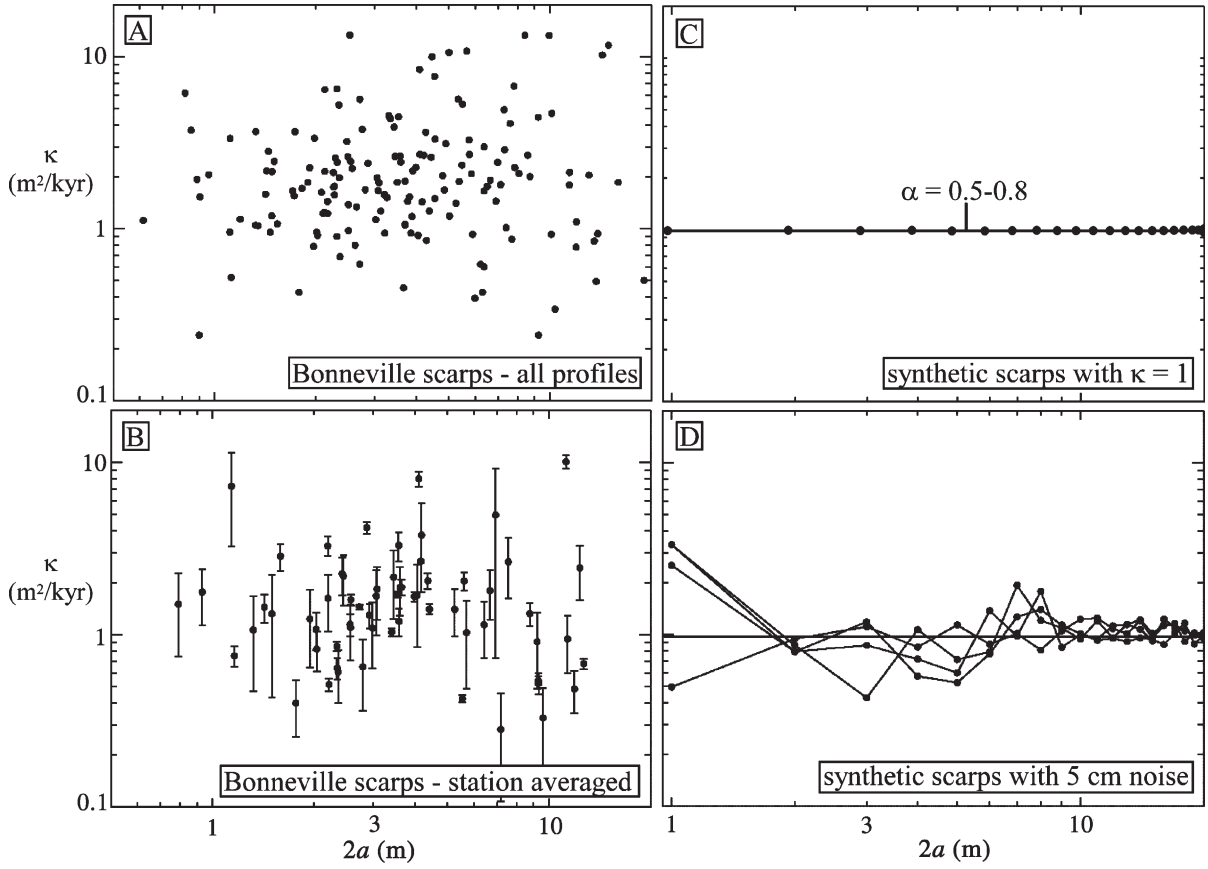

Fig. 7. Diffusivity values inferred from full-scarp-fitting method. (A) All Bonneville scarps. (B) Bonneville scarps, station-averaged (error bars represent standard deviation of diffusivity values between different profiles at the same station). (C) Analytic solutions of the diffusion equation with $\kappa = 1$ m^2/kyr, $T = 10$ kyr, and a range of scarp heights ($2a = 1$–20 m) and initial gradients ($\alpha - b = 0.4$–0.7), and (D) analytic solutions (same as C) with small-scale (5-cm root-mean-squared) random variability superimposed.

occurs for $\alpha - b = 0.70$, the solution is essentially independent of the reduced initial gradient. This makes physical sense because, for a short, narrow scarp, diffusive smoothing quickly reduces the maximum slope to a value far below the angle of repose. For a tall, broad scarp (Fig. 6B), however, the scarp form is sensitive to the initial angle. The best-fit model parameters in this case have well-defined values for both diffusion age and reduced initial gradient ($\kappa = 0.78$ m^2/kyr and $\alpha - b = 0.48$). Physically, fitting the full scarp works best because the scarp profile contains independent information about the diffusion age and the initial gradient. The diffusion age is determined primarily by the width of the slope break at the top and bottom of the scarp. The reduced initial gradient is determined by the shape of the flat, central portion of the gradient profile shown in Fig. 6B (also shown in the analytic solutions of Fig. 3C).

Fig. 7 illustrates the results of the full-scarp method for the Bonneville scarp database and the synthetic profiles considered in Section 4.2. For the Bonneville scarps, the data have been plotted in two ways: Fig. 7A illustrates all of the scarps, and Fig. 7B illustrates the data averaged by station. Station averaging was performed by computing the average and standard deviation of the κ values obtained for all of the profiles acquired at a given station (between two and four profiles). Diffusivity values in Fig. 7A and B show no systematic change with scarp height, indicating no evidence for nonlinear scarp processes to within the uncertainty inherent in the analysis. It should be noted that Mattson and Bruhn (2001), also using full-scarp methods, presented evidence for nonlinear evolution of the Bonneville shoreline for scarps between 20 and 30 m tall. Their study, however, included data from only four stations. Analysis of our larger data set from west-central Utah provides results fully consistent with linear diffusion up to 20 m in height, but scarps taller than 20 m could not be evaluated because none were present in the study area.

The results of the full-scarp method on analytic solutions of the diffusion equation are shown in Fig. 7C (without noise) and Fig. 7D (with noise). Fig. 7C illustrates that the method returns the exact result ($\kappa = 1$ m^2/kyr) for all scarp heights and initial gradients. This is an ideal result, signifying that the method is unbiased and can "detect" the initial gradient in the profile and separate its effect from that of the diffusion age. In the presence of noise (Fig. 4D), the method shares the limited signal-to-noise ratio of all short scarps, but the variability in diffusivity values decreases steadily with increasing scarp height.

The full-scarp method can also be applied to the lower and upper half of the scarp separately. There are several reasons why diffusivity values might differ between the two halves of a scarp. Preferential transport of fine-grained material from the top half of the scarp to the lower half, for example, could lead to progressive armoring of the top portion of the scarp and hence lower diffusivity values. Similarly, petrocalcic or argillic soil horizons near the upper surface could cause lower diffusivity values at the top half of the scarp relative to the bottom half. Fig. 8A illustrates the diffusivity values for the top and bottom halves, indicating that, in fact, there is no significant difference. The histogram of diffusivity values, plotted in Fig. 8B, further illustrates that result. A Kolmogorov–Smirnov test (Press et al., 1992) confirmed that the two distributions were not distinct to even a 50% confidence level.

The influence of scarp orientation and texture on diffusivity values of the Bonneville scarps is evaluated in Fig. 9. Fig. 9A plots diffusivity values as a function

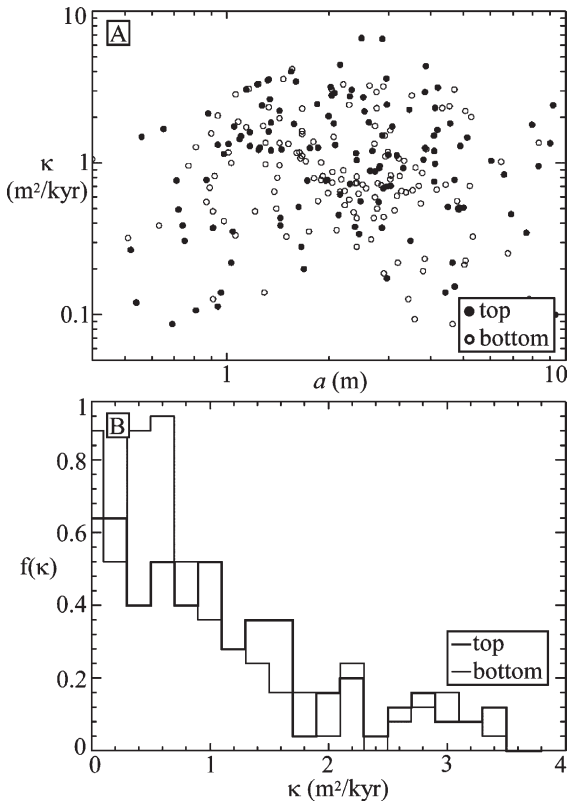

Fig. 8. (A) Diffusivity values obtained by dividing each profile into a top and bottom half and performing scarp analysis separately on each half. (B) Histogram of diffusivity values (from $\kappa = 0$–4 m^2/kyr), for scarp tops and bottoms. Neither the mean nor the distribution of diffusivity values shows a significant difference between the top and bottom of the scarp.

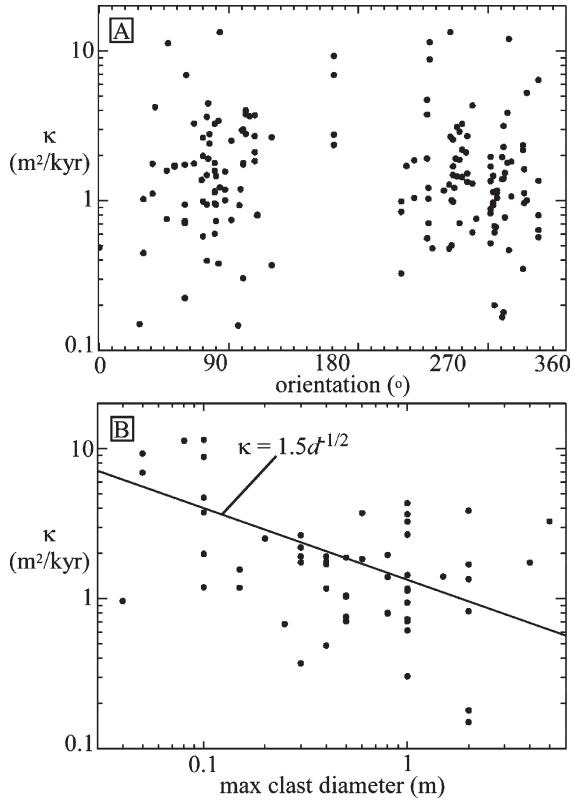

Fig. 9. Diffusivity values plotted as a function of scarp (A) orientation (0° is due east) and (B) texture, characterized by maximum clast diameter. No significant relationship was found between diffusivity values and orientation. Diffusivity values have a weak but significant inverse relationship with maximum clast diameter. The best-fit relationship is $\kappa = 1.5d^{-1/2}$, but with a great deal of scatter.

of scarp orientation. No significant trend can be detected. The relationship between diffusivity and maximum clast diameter (Fig. 9B) shows a weak but significant inverse trend at the 85% confidence level. This inverse trend suggests that coarse-grained alluvial-fan deposits evolve more slowly than fine-grained deposits, and it provides a preliminary quantitative relationship between the two variables. A least-square fit to the data in Fig. 9B (note the logarithmic scales) suggests that diffusivity values and maximum texture are related by

$$\kappa = \kappa_0 d^{-0.5} \tag{8}$$

where d is equal to the maximum clast diameter, and $\kappa_0 = 1.5$ m^2/kyr for this climatic region. It should be noted that many other functions could be fit to the data, and Eq. (8) represents only one possible form. Eq. (8) provides a preliminary means of incorporating soil texture into regional calibrations of diffusivity values needed for paleoseismic studies. In addition to measuring maximum clast diameter, we also recorded the mean clast diameter from an average of 100 surface clasts. Mean clast diameter is not representative of the underlying parent material, however, because it predominantly reflects desert-pavement processes acting on the surface. As a result, we found no significant correlation between diffusivity values and mean clast diameter.

5. Discussion

To help interpret the results of Fig. 9, we must first identify the predominant hillslope processes acting on gravelly scarps in west-central Utah. The absence of significant armoring and asymmetry in the Bonneville scarps (Fig. 8) suggests that the predominant hillslope processes are capable of transporting fine- and coarse-grained material with roughly equal efficiency. Rainsplash and slope wash, while potentially important for transporting fine-grained sediment locally, are unlikely to influence the scarp as a whole for this reason. Field observations on small-scale disturbances associated with plant mounds and animal burrowing suggest that floral and faunal bioturbation are, together with creep, the predominant hillslope processes in the area.

If floral bioturbation is important, then the absence of microclimatic control seems, at first, to be a very surprising result. Slope orientation clearly influences mean vegetation density throughout the Basin and Range, i.e., north-facing slopes have lower evapotranspiration rates and, hence, higher vegetation density in arid and semi-arid climates of the northern hemisphere. Therefore, one might expect that floral bioturbation rates must be greater on north-facing slopes. The driving factor in floral bioturbation, however, is the turnover in vegetation cover, not the vegetation cover itself. As a result, north-facing slopes may have a higher mean vegetation cover but fewer life cycles. The results of Fig. 9A suggest that any increase in bioturbation rates associated with higher mean vegetation densities are offset by lower turnover rates in these microclimates. As a caveat, scarp orientation may, in fact, be a significant influence on scarp evolution but undetectable given the inherent variability in scarp profiles illustrated by the large scatter in Figs. 7–9.

6. Conclusion

The results of this study indicate that scarp evolution in west-central Utah is consistent with the linear diffusion equation for scarps 20 m or less in height, with no variation in diffusivity values with scarp orientation. Diffusivity values also do not differ between the tops

and bottoms of scarps, but they do have a weakly significant inverse relationship with texture. These results are broadly consistent with the observation that bioturbation and creep are the predominant hillslope processes acting on these scarps. Our systematic study of scarp-analysis methods has highlighted the importance of analyzing the full scarp profile in order to maximize the information content of each scarp. Full-scarp analysis that incorporates a range of initial gradients is the most accurate and robust method for scarp analysis on a profile-by-profile basis. The inherent uncertainty remaining in scarps, however, is quite significant and can lead to an order-of-magnitude variation in diffusion age. This uncertainty appears to be a combination of random spatial variability in hillslope evolution and small-scale disturbances in the modern scarp profile.

Acknowledgements

We thank Ramon Arrowsmith and an anonymous reviewer for very constructive reviews. This work was supported by the Department of Geosciences, University of Arizona, through course Geosciences 650, Field Studies in Geomorphology, and NSF grant EAR-0309518.

References

Andrews, D.J., Bucknam, R.C., 1987. Fitting degradation of shoreline scarps by a nonlinear diffusion model. Journal of Geophysical Research 92, 12857–12867.

Andrews, D.J., Hanks, T.C., 1985. Scarp degraded by linear diffusion: inverse solution for age. Journal of Geophysical Research 90, 10193–10208.

Arrowsmith, J.R., Rhodes, D.D., Pollard, D.D., 1998. Morphologic dating of scarps formed by repeated slip events along the San Andreas Fault, Carrizo Plain, California. Journal of Geophysical Research 103, 10141–10160.

Avouac, J.-P., 1993. Analysis of scarp profiles: evaluation of errors in morphologic dating. Journal of Geophysical Research 98, 6745–6754.

Avouac, J.-P., Peltzer, G., 1993. Active tectonics in southern Xingiang, China: analysis of terrace riser and normal fault scarp degradation along the Hotan–Qira fault system. Journal of Geophysical Research 98, 21773–21807.

Bucknam, R.C., Anderson, R.E., 1979. Estimation of fault-scarp ages from a scarp-height-slope-angle relationship. Geology 7, 11–14.

Carson, M.A., Kirkby, M.J., 1972. Hillslope Form and Process. Cambridge University Press, New York, NY.

Culling, W.E.H., 1960. Analytical theory of erosion. Journal of Geology 68, 336–344.

Culling, W.E.H., 1963. Soil creep and the development of hillside slopes. Journal of Geology 71, 127–161.

Enzel, Y., Amit, R., Harrison, J.B.J., Porat, N., 1994. Morphologic dating of fault scarp and terrace risers in the southern Arava, Israel: comparison to other dating techniques and implication for paleoseismicity in the southern Arava, Israel. Israel Journal of Earth-Sciences 43, 91–103.

Furbish, D.J., Haff, P.K., 1999. The master equation applied to landscape evolution. Abstracts with Programs-Geological Society of America 31, 255.

Hallet, B., Putkonen, J.K., 1994. Surface dating of dynamic landforms: young boulders on aging moraines. Science 265, 937–940.

Hanks, T.C., 2000. The age of scarplike landforms from diffusion equation analysis. In: Noller, J.S., Sowers, J.M., Lettis, W.R. (Eds.), Quaternary Geochronology, Methods and Applications. American Geophysical Union, Washington, DC, pp. 313–338.

Hanks, T.C., Andrews, D.J., 1989. Effect of far-field slope on morphologic dating of scarplike landforms. Journal of Geophysical Research 94, 565–573.

Hanks, T.C., Wallace, R.E., 1985. Morphological analysis of the Lake Lahontan shoreline and beach-front fault scarps, Pushing County, Nevada. Bulletin of the Seismological Society of America 75, 835–846.

Hanks, T.C., Buckman, R.C., Lajoie, K.R., Wallace, R.E., 1984. Modification of wave-cut and faulting-controlled landforms. Journal of Geophysical Research 89, 5771–5790.

Heimsath, A.M., Dietrich, W.E., Nishiizumi, K., Finkel, R.C., 1997. The soil production function and landscape equilibrium. Nature 388, 358–361.

Hsu, L., Pelletier, J.D., 2004. Correlation and dating of Quaternary alluvial-fan surfaces using scarp diffusion. Geomorphology 60, 319–335.

Jyotsna, R., Haff, P.K., 1997. Microtopography as an indicator of modern hillsope diffusivity in arid terrain. Geology 25, 695–698.

Martin, Y., 2000. Modelling hillslope evolution; linear and nonlinear transport relations. Geomorphology 34, 1–21.

Mattson, A., Bruhn, R.L., 2001. Fault slip rates and initiation age based on diffusion equation modeling: Wasatch fault zone and eastern Great Basin. Journal of Geophysical Research 106, 13739–13750.

Mayer, L., 1984. Dating Quaternary fault scarps formed in alluvium using morphometric parameters. Quaternary Research 22, 300–313.

McKean, J.A., Dietrich, W.E., Finkel, R.C., Southon, J.C., Caffee, M.W., 1993. Quantification of soil production and downslope creep rates from cosmogenic ^{10}Be accumulations on a hillslope profile. Geology 21, 343–346.

Nash, D.B., 1980a. Morphologic dating of degraded normal fault scarp. Journal of Geology 88, 353–360.

Nash, D.B., 1980b. Forms of bluffs degraded for different lengths of time in Emmet County, Michigan, USA. Earth Surface Processes 5, 331–345.

Nash, D.B., 1984. Morphologic dating of fluvial terrace scarps and fault scarps near West Yellowstone, Montana. Geological Society of America Bulletin 95, 1413–1424.

Nash, D.B., 1998. Influence of scarp height on the accuracy of morphologic dating. Abstracts with Programs-Geological Society of America 30, 329.

Oviatt, C.G., Currey, D.R., Sack, D., 1992. Radiocarbon chronology of Lake Bonneville, Eastern Great Basin. Palaeogeography, Palaeoclimatology, Palaeoecology 99, 225–241.

Pearthree, P.A., Calvo, S.S., 1987. The Santa Rita fault zone: evidence for large magnitude earth-quakes with very long recurrence intervals, Basin and Range province of southeastern Arizona. Bulletin of the Seismological Society of America 77, 97–116.

Pierce, K.L., Colman, S.M., 1986. Effect of height and orientation (microclimate) on geomorphic degradation rates and processes,

late-glacial terrace scarps in central Idaho. Geological Society of America Bulletin 97, 869–885.

Press, W.H., Flannery, B.P., Teukolsky, S.A., Vetterling, W.T., 1992. Numerical Recipes in C, 2nd ed. Cambridge University Press, New York, NY.

Reheis, M., 1999. Extent of Pleistocene Lakes in the Western Great Basin. U.S. Geological Survey Miscellaneous Field Studies Map MF-2323. U.S. Geological Survey, Denver, CO.

Roering, J.J., Kirchner, J.W., Dietrich, W.E., 1999. Evidence for non-linear, diffusive sediment transport and implications for landscape morphology. Water Resources Research 35, 853–870.

Sack, D., 1990. Quaternary Geology of Tule Valley, West-Central Utah. Utah Geological and Mineral Survey Map 124, scale 1:100,000.

Simons, D.B., Albertson, M.E., 1963. Uniform water conveyance channels in alluvial material. Transactions of the American Society of Civil Engineers 128, 65–108.

Wallace, R.E., 1977. Profiles and ages of young fault scarps, north-central Nevada. Geological Society of America Bulletin 88, 1267–1281.